Design of a folded, multi-pass Fabry–Perot cavity for displacement metrology

2009 Meas. Sci. Technol. 20 107001

(http://iopscience.iop.org/0957-0233/20/10/107001)

Meas. Sci. Technol. **20** (2009) 107001 (5pp) doi:10.1088/0957-0233/20/10/107001

TECHNICAL DESIGN NOTE

Design of a folded, multi-pass Fabry–Perot cavity for displacement metrology

Ki-Nam Joo, Jonathan D Ellis, Jo W Spronck and Robert H Munnig Schmidt

Mechatronic System Design, Department of Precision and Microsystems Engineering, Delft University of Technology, Delft, The Netherlands

E-mail: k.joo@tudelft.nl

Received 7 July 2009, in final form 28 July 2009
Published 9 September 2009
Online at stacks.iop.org/MST/20/107001

Abstract

We present a folded, multi-pass cavity design for displacement measuring Fabry–Perot interferometry. The cavity length is designed to be one-quarter of the physical length needed for a typical Fabry–Perot interferometer by using a quarter-wave plate and a retroreflector. This enhances the displacement sensitivity by a factor of four, allowing for higher resolution in viewing the effects caused by mechanical motions, refractive index changes and frequency fluctuations from the laser source. Furthermore, the geometrical error motions are minimized by using a retroreflector due to its tip–tilt insensitivity. In this note, a theoretical analysis of the folded, multi-pass Fabry–Perot cavity is described and analyzed with Jones matrices in ideal and non-ideal designs.

Keywords: Fabry–Perot interferometer, displacement, cavity design

(Some figures in this article are in colour only in the electronic version)

1. Introduction

The demand for high precision is increasing because industry is requiring tighter tolerances for dimensional metrology systems. Moreover, measurements should be traceable to the length standard because it allows for a proper assessment of measurement uncertainty. Fabry–Perot (FP) interferometry for displacement measurements potentially has sub-nanometer uncertainty and traceability to length standards [1]. This can be achieved because displacements are converted into an optical frequency change which can be compared with standard frequency-stabilized lasers such as an iodine stabilized helium–neon (He–Ne) laser or a stabilized frequency comb. Because of these characteristics, traceable FP interferometry has been used for metrology in atomic force microscopy [2] and as a calibration instrument for capacitive or inductive sensors [1, 3]. Additionally, FP interferometry is efficient in detecting the periodic errors in homodyne and heterodyne displacement interferometers [4].

A FP cavity consists of two highly reflecting surfaces, typically one flat and one concave mirror (M), which helps create multiple interferences. The optical frequency of a tunable laser can be locked to a resonance peak of the FP cavity and the locked frequency is shifted when one cavity mirror is moved [1–4]. From this, the displacement can be calculated using the nominal cavity length and the calibrated optical frequency. In principle, a tunable laser source and a stabilized optical frequency standard are necessary to measure the frequency shifts in FP interferometry. An external cavity laser diode (ECLD) with 635 nm wavelength is an attractive, tunable source due to its wide tunable range ($\sim$10 nm) and its narrow linewidth. The frequency shift can be measured with an iodine stabilized He–Ne laser up to a few tens of GHz, which is dependent on the bandwidth of the photodetector (PD) used, so the displacements can be measured continuously without any fly back states in the range of a few micrometers [2]. However, the use of an ECLD and high-speed PD is limited in some industrial and research applications due to its high cost.

In comparison, using a He–Ne laser is an attractive solution because it has low cost and high reliability. Additionally, a He–Ne based FP interferometer is directly traceable to length standards when compared with an iodine stabilized He–Ne laser. The major drawback of using He–Ne lasers is that the tunable range of the He–Ne laser is rather narrow, only approximately 1.5 GHz. In this case, the free spectral range (F.S.R.) of the FP cavity should be narrower than the gain bandwidth of the He–Ne laser for the locking and unlocking technique to measure long displacements [1]. Therefore, this leads to using long cavities because of the narrow bandwidth, which are undesirable because they decrease the stability of the system caused by mechanical vibrations, laser frequency instabilities and refractive index changes [2].

In this note, we describe a simple, practical FP cavity, which allows a He–Ne laser as an optical source with effectively four times the physical length of a typical FP cavity with the same F.S.R. This modified cavity increases the sensitivity of the system, providing higher precision measurements. Additionally, the cavity alignment is decoupled from the displacement alignment, making the system insensitive to rotational misalignments during motions. The design is based on multiple optical paths inside the cavity using a retroreflector (RR) and a quarter-wave plate (QWP), so the actual cavity length is not changed. Mathematical analyses were performed to assess the ideal behavior of this modified cavity architecture, as well as its sensitivity to polarization effects and misalignment in non-ideal measurements.

2. Fabry–Perot interferometer for displacement measurements

In the typical, traceable FP interferometer configuration for displacement measurements, the light from a tunable optical source travels into a cavity which consists of two mirrors. The frequency of the source is locked to the resonance frequency of the cavity and is shifted by displacing one mirror. Then the frequency shifts can be measured by comparing this signal with a frequency-stabilized laser [1–4]. The FP interferometer is based on the multiple interferences between the two cavity mirrors, and the transmittance can be expressed with the cavity length (L) as [5]

$$\frac{I_t}{I_i} = \frac{T^2}{(1+R^2) - 2R\ \cos(2kL)}, \tag{1}$$

where I_t and I_i are the intensities for the transmitted beam and the incident beam, R and T are the intensity reflectance and transmittance of the cavity mirrors, respectively, and k is the wave number of the light in the medium inside the cavity. If the optical frequency (f) of the source is locked to one of these resonance frequencies and one cavity mirror is moved with the displacement of ΔL, then, the frequency shift (Δf) becomes [1]

$$\Delta f = -\frac{\Delta L}{L} f. \tag{2}$$

Because Δf can easily be measured with respect to a frequency-stabilized laser, ΔL can be determined based on the nominal cavity length and the optical frequency using equation (2). For example, a frequency shift of 100 kHz is a cavity length change of 32 pm with a He–Ne laser (632.8 nm) and 150 mm cavity length.

An important issue to be considered in a FP interferometer is the relation between the F.S.R. ($= c/2nL$) of the FP cavity and the tunable range of the laser source. When using a He–Ne laser as the optical source, the tunable range is the gain bandwidth of the He–Ne medium, which is approximately 1.5 GHz. In order to measure displacements continuously, the laser source must be locked to the next resonance peak of the cavity before a mode hop occurs in the laser [1]. This means the F.S.R. of the cavity should be narrower than 1.5 GHz because the peak needs to be in the gain bandwidth of the He–Ne laser. From this, the cavity length must be longer than 100 mm which is a F.S.R. of 1.5 GHz in air. When the cavity length is longer, however, the stability decreased due to mechanical vibrations, laser frequency instabilities, refractive index changes [2] and thermal gradients. Additionally, the cost of the system is increased because thermally stable materials are needed and the environment in the system needs to be monitored and controlled.

3. QWP-based, folded FP cavity

In many optical applications, it is possible to shorten optical paths or simplify optical configurations by using polarization optics. The modified FP cavity design is based on the polarization characteristics of light and polarizing optics. Figure 1 shows the optical configuration of the FP interferometer using a modified cavity with a QWP and a RR instead of a mirror to enhance the displacement sensitivity. The light from the source passes though an optical isolator (OI) where the output polarization is not entirely vertical or horizontal. This beam then passes through a polarizing beam splitter (PBS) and is split into two beams. The reflected beam travels to an avalanche photodetector (APD) where it interferes with a beam from the frequency-stabilized laser to detect the frequency shifts. The transmitted beam from the PBS travels to the FP cavity which consists of a coated QWP rotated at 45° with respect to the PBS, a RR and a concave mirror. The QWP is coated with high reflection coating at the first surface so the first reflected beam from the QWP passes back to the optical source and is blocked by the OI. The transmitted beam from the QWP goes to the RR, the M and then back to the QWP again. In this case, the transmitted beam from the QWP is reflected by the PBS and detected with a PD because the beam passes through the QWP twice, changing its polarization state. Because of the QWP, the beam leaving the FP cavity will alternate between being blocked by the OI and being detected by the PD. Essentially, a beam must travel through the FP cavity an odd number of times in order to be detected

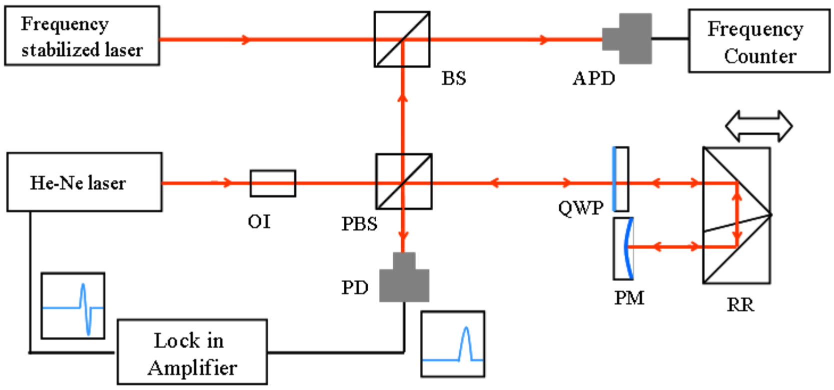

Figure 1. Optical configuration of FP interferometer with the multiple-pass FP cavity; OI: optical isolator, BS: beam splitter, PD: photo detector, APD: avalanche photodetector, PBS: polarizing beam splitter, QWP: quarter-wave plate, RR: retro-reflector, PM: parabolic mirror.

by the PD. These odd-numbered beams create the multiple interference signal from the FP interferometer.

Consequently, the effective length of this QWP-based, folded FP cavity is four times the geometric cavity length, which increases the displacement sensitivity by a factor of four. Thus, the F.S.R. of this cavity is the same as a conventional FP cavity with four times this length. The main advantage of this modified cavity is that it can be more compact, making it less susceptible to thermal gradients, and thus, its own mechanical stability. The length change from refractive index change inside the modified cavity is also less sensitive than a corresponding length change from the same refractive index change in a conventional cavity [6]. This is due to the four-fold increase in sensitivity. Additionally, the cavity can be separated from the detector because the input beam and the measurement beam are both located on the same side of the cavity. This can allow the FP interferometer to be more closely integrated into a system because access to both sides of the cavity is not needed. Moreover, the RR can compensate tip and tilt error motions, so the geometrical motion errors can be reduced [7].

4. Mathematical analysis

A Jones matrix model was implemented to analyze the system parameters such as the F.S.R., sensitivity and the linewidth of the peak in the modified FP cavity. The Jones matrices for a QWP ($\overline{Q}$), transmittance ($\overline{\mathrm{PBS}_t}$) and reflection ($\overline{\mathrm{PBS}_r}$) in a PBS are applied in this analysis, and the electric field ($\overline{E_o}$) from the PD can be described as

$$\overline{E_o} = (\overline{\mathrm{PBS}_r})\overline{M}(\overline{\mathrm{PBS}_t})\overline{E_i}, \tag{3}$$

where $\overline{E_i}$ is the electric field of the source, and $\overline{M}$ is a transformation matrix of the FP cavity [8]. The expression for the transformation matrix of the p-pass inside the cavity is

$$\begin{aligned}\bar{M} &= -r\bar{I} - t^2r^3d^4\bar{R}^{-1}\bar{Q}^2\bar{R} + t^2r^7d^8\bar{R}^{-1}\bar{Q}^4\bar{R} \\ &\quad - t^2r^{11}d^{12}\bar{R}^{-1}\bar{Q}^6\bar{R} + \cdots \\ &= -r\bar{I} + t^2r^3d^4\sum_{p=1}^{\infty}(-1)^p(rd)^{4(p-1)}\bar{R}^{-1}\bar{Q}^{2p}\bar{R},\end{aligned} \tag{4}$$

where r and t mean the reflectance and transmittance coefficients of the mirrors, d is denoted by $\mathrm{e}^{-\mathrm{i}kL}$, which is a phase change caused by the cavity length, $\bar{R}$ is a rotation matrix with the angle between the main axes of the PBS and QWP, and $\bar{I}$ is an identity matrix for the electric fields. Then, $\overline{E_o}$ can be rewritten by equations (3) and (4) as

$$\overline{E_o} = \begin{pmatrix} A_x\,\mathrm{e}^{\mathrm{i}\delta_x}(-r + S_1\cos^2\theta + S_2\sin^2\theta) & (S_1 - S_2)\sin\theta\cos\theta \\ A_xA_y\,\mathrm{e}^{\mathrm{i}(\delta_x+\delta_y)}(S_1 - S_2)\sin\theta\cos\theta & A_y\,\mathrm{e}^{\mathrm{i}\delta_y}(-r + S_1\sin^2\theta + S_2\cos^2\theta)\end{pmatrix}\overline{E_i}, \tag{5}$$

where $S_1 = \frac{-t^2r^3d^4B_x^2\,\mathrm{e}^{-\mathrm{i}(\pi/2+\varphi)}}{1+r^4d^4B_x^2\,\mathrm{e}^{-\mathrm{i}(\pi/2+\varphi)}}$, $S_2 = \frac{-t^2r^3d^4B_y^2\,\mathrm{e}^{\mathrm{i}(\pi/2+\varphi)}}{1+r^4d^4B_y^2\,\mathrm{e}^{\mathrm{i}(\pi/2+\varphi)}}$ and θ is the angle between the main axes of the PBS and QWP. A_x, A_y are the leakage coefficients of other polarizations and δ_x, δ_y mean the phase changes between the main axes of the transmitted and reflected beams from the PBS, respectively. B_x, B_y are the transmittance coefficients of the QWP main axes, and φ is the phase error of the QWP.

For an ideal case ($A_x = A_y = \delta_x = \delta_y = \varphi = 0$, $B_x = B_y = 1$, $\theta = \pi/4$) with a vertically polarized input beam, the intensity (I_o) obtained by the PD can be expressed as

$$I_o = \frac{(1-R)^2R^3}{(1+R^8) + 2R^4\cos 8kL}I_i, \tag{6}$$

where R is the intensity reflectance of the mirror surface and denoted by r^2. Figure 2 shows the intensity ratio between the input and output beams according to the phase. One significant difference in the modified cavity is the peak intensities, which are decreased by a factor of four due to losses in the PBS and only using a single polarization state. The first reflected beam from the QWP as well as other transmitted beams by the PBS does not travel to the PD; therefore, the total intensity at the PD is reduced. However, the F.S.R. of the modified FP cavity becomes one quarter of the F.S.R. in a traditional cavity with the same length. As shown in figure 2 and equation (6), the peaks appear at a phase of ($\pi + 2m\pi$) and the peak frequency in the frequency domain is

$$\nu_m = \frac{c}{16nL} + \frac{mc}{8nL}, \tag{7}$$

where ν_m is the resonance peak frequency of the FP cavity. The F.S.R. can subsequently be expressed as

$$\mathrm{F.S.R.} = \nu_{m+1} - \nu_m = \frac{c}{8nL}. \tag{8}$$

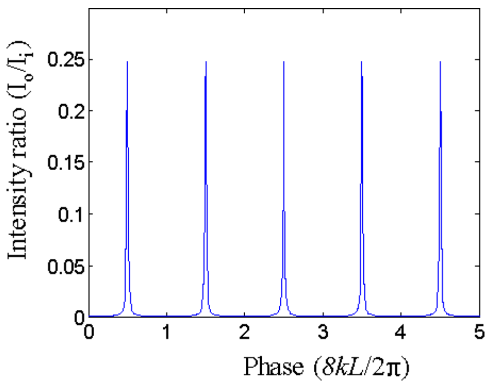

Figure 2. Intensity ratio between the input and the output beams of the modified FP cavity.

This modified cavity length of L is comparable to a typical cavity with a nominal length of $4L$. For example, we will assume the FP cavity has a length change of 1 nm and it uses a He–Ne laser as the source, which has a nominal frequency of approximately 474 THz. This will be compared across three different FP cavities—traditional cavities with lengths of 40 mm and 160 mm and the modified cavity with a length of 40 mm. In the case of a 160 mm long traditional FP cavity, the F.S.R. is calculated as 937.5 MHz, which is narrower than the gain bandwidth of the He–Ne laser (1.5 GHz), so the FP interferometer can be operated successfully. However, the F.S.R. of the 40 mm long traditional FP cavity is 3.75 GHz, which makes using a He–Ne laser difficult. The F.S.R. of the 40 mm long, QWP-based, folded FP cavity is 935.7 MHz, which means it is possible to use a He–Ne laser as the source and have the FP interferometer work effectively.

When comparing the frequency shift induced by a 1 nm nominal length change, the 160 mm long traditional cavity has a shift of 2.96 MHz. However, the 40 mm long cavities, both traditional and modified, have frequency shifts of 11.85 MHz. This is because the frequency shift is inversely proportional to the nominal length of the traditional cavity from equation (2) and the length change is multiplied in the modified cavity. From this, the sensitivity of the FP interferometer with the modified cavity is four times better than that of the typical FP interferometer using the long cavity.

Another important parameter in the FP cavity is the linewidth of a measured intensity peak. This affects the sensitivity of the locking signal and the frequency range of locking. The original linewidth ($\Delta\nu_{\mathrm{TFP}}$) of the transmitted intensity peak in a FP cavity (full width at half maximum, FWHM) can be determined with the cavity length and the intensity reflectance of the mirror (R) by

$$\Delta\nu_{\mathrm{TFP}} = \frac{c}{2nL} \times \frac{(1-R)}{\pi\sqrt{R}}. \tag{9}$$

On the other hand, the linewidth ($\Delta\nu_{\mathrm{MFP}}$) of the output intensity peak in the QWP FP cavity is calculated by

$$\Delta\nu_{\mathrm{MFP}} = \frac{c}{8nL} \times \frac{(1-R^4)}{\pi R^2}. \tag{10}$$

Assuming the same cavities described earlier and that R is a reflectance of 99.5%, $\Delta\nu_{\mathrm{TFP}}$ of the traditional short and

Table 1. Calculated results of the F.S.R., the frequency shift of 1 nm length change and the linewidth of the intensity peak for 40 mm FP cavity, modified cavity and 160 mm FP cavity at $R = 0.995$.

	40 mm long traditional FP (MHz)	160 mm long traditional FP (MHz)	40 mm long QWP-based, folded cavity (MHz) (effective length = 160 mm)
F.S.R.	3750	937.5	937.5
Frequency shift ($\Delta L = 1$ nm)	11.85	2.96	11.85
Linewidth	5.98	1.49	5.98

long cavities is 1.49 MHz and 5.98 MHz, respectively. In the modified cavity, $\Delta\nu_{\mathrm{MFP}}$ is 5.98 MHz. Because the beam incident on the modified cavity is additionally reflected by the RR compared to the typical cavity, the sharpness of the peak is reduced. Additionally, the intensity is one quarter of the nominal value because a PBS is used. This large linewidth can limit the locking stability in the electrical control system because the locking stability is related to the zero stability of the electronics and the linewidth of the cavity [1]. For a fixed zero stability in the electronics, the locking stability is proportional to the linewidth of the cavity; therefore, a narrower linewidth is optimal for better locking stability. In FP interferometry, the linewidth of the cavity could be adjusted with the intensity reflectance of the mirrors and the RR for high locking stability. Table 1 shows the characteristics of the F.S.R., frequency shift and linewidth of the peak for each cavity.

To summarize, the multiple-pass FP cavity can be used for FP interferometry using a He–Ne laser instead of a long cavity. Moreover, it can improve the displacement sensitivity from effects caused by mechanical vibration and thermal gradients because of the short cavity length. Additionally, displacements in the cavity are insensitive to misalignment because a RR is used as the moving element and the shorter cavity is less susceptible to errors caused by refractive index fluctuations. Frequency fluctuations from the He–Ne source have less of an effect on the measured displacement change based on equation (2). Although the linewidth of the peak is broad compared to a traditional, long cavity, this can be overcome by using highly reflective mirrors and a stable electronic locking system.

5. Imperfect QWP-based, folded FP cavity

In practical cases, the characteristics of the multiple-pass FP cavity are affected by the alignment and actual transmittance characteristics of each optical component, which are shown in equation (5). The phase errors and alignment errors of the QWP and PBS can significantly affect the results. Among them, the most important parameters are the transmittance and the phase errors of the QWP while the others only affect the peak intensity. The transmittance of the QWP (B_x, B_y) affects the peak intensity value and the linewidth

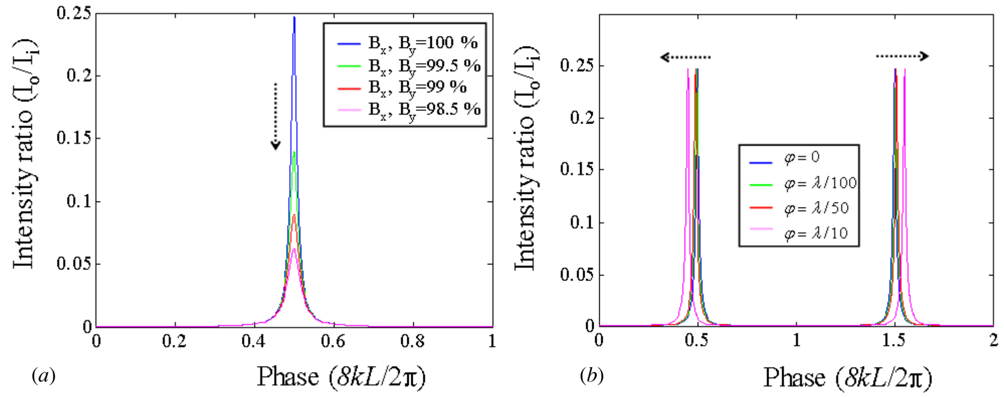

Figure 3. Output intensity ratio change of the modified cavity with (*a*) transmittance and (*b*) phase error of the QWP.

of the peak in the output. Figure 3(*a*) shows the output intensity ratio changes of the modified cavity with the variable transmittance ratio of the QWP. As the transmittance of the QWP decreases, the output intensity is lower due to the intensity loss inside the cavity. The linewidth, which is a function of the reflectance *R*, becomes broader because the low transmittance of the QWP effectively leads to low *R* in equation (10).

The phase errors of the QWP result in the phase change of the intensity peak as shown in figure 3(*b*). An interesting phenomenon is that the peaks have bi-directional motions, i.e. the odd peaks and even peaks move in opposite directions. Assuming a phase error of $\lambda/300$, which can be achieved in high-quality QWPs, and a 40 mm cavity, the frequency shifts of the peaks are ± 4.68 MHz. However, the frequency shift caused by the phase errors of the QWP is fixed and it does not cause any errors for basic FP interferometer operation. Provided the environmental effects can be limited over a short time period and the laser frequency change occurs relatively fast, these bi-direction peaks could be mapped, thus backing out the initial misalignment, allowing for further correction. One aspect not modeled is the polarization effects in the RR. However, these effects can be minimized by using a hollow RR, which not only has a higher reflectance than a standard glass RR and two less surfaces to pass through, but also creates less polarization error [9].

6. Conclusion

In this note, a QWP-based, folded Fabry–Perot cavity design for Fabry–Perot interferometry using a He–Ne laser source was presented. The purpose of this design is to reduce the cavity length and enhance the sensitivity of the FP interferometer. The QWP-based, folded FP cavity consists of a retroreflector which compensates the tilt motions during displacements and a quarter-wave plate to adjust the polarization state of the light. The effective length of this modified cavity is four times the geometric cavity length and the displacement sensitivity is four times more than a traditional cavity.

A theoretical analysis of the FP interferometer was presented using Jones matrices and compared to typical Fabry–Perot cavities in ideal and practical cases. While the nominal peak intensity is decreased and the linewidth is increased by a factor of four, this modified cavity has higher displacement sensitivity and can be remotely located because access to both sides of the cavity is not needed. This note can give some preliminary information and insight into designing Fabry–Perot cavities with improved sensitivity over traditional cavity designs.

Acknowledgments

This work was supported by the Dutch IOP under the projects IPT004001 and IPT06104.

References

[1] Haitjema H, Schellekens P H J and Wetzels S F C L 2000 Calibration of displacement sensors up to 300 μm with nanometre accuracy and direct traceability to a primary standard of length *Metrologia* **37** 25–33

[2] Howard L, Stone J and Fu J 2001 Real-time displacement measurements with a Fabry–Perot cavity and a diode laser *Precis. Eng.* **25** 321–35

[3] Wetzels S F C L and Schellekens P H J 1997 Development of a traceable laser-based displacement calibration system with nanometer accuracy *Ann. CIRP* **46** 481–4

[4] Cosijns S J A G, Haitjema H and Schellekens P H J 2003 Traceable calibration of non-linearities in laser interferometers *Ann. ASPE* **30** 307–10

[5] Yariv A 1988 *Quantum Electronics* 3rd edn (New York: Wiley)

[6] Haitjema H, Rosielle P C J N, Kotte G and Steijaert H 1998 Design and calibration of a parallel-moving displacement generator for nano-metrology *Meas. Sci. Technol.* **9** 1098–104

[7] Mao W, Zhang S, Cui L and Tan Y 2006 Self-mixing interference effects with a folding feedback cavity in Zeeman-birefringence dual frequency laser *Opt. Express* **14** 182–9

[8] Gerrard A and Burch J M 1975 *Introduction to Matrix Methods in Optics* (New York: Wiley)

[9] Kalibjian R 2004 Stokes polarization vector and Mueller matrix for a corner-cube reflector *Opt. Commun.* **240** 39–68